

We are IntechOpen, the world's leading publisher of Open Access books Built by scientists, for scientists

6,900

Open access books available

186,000

International authors and editors

200M

Downloads

Our authors are among the

154

Countries delivered to

TOP 1%

most cited scientists

12.2%

Contributors from top 500 universities



WEB OF SCIENCE™

Selection of our books indexed in the Book Citation Index
in Web of Science™ Core Collection (BKCI)

Interested in publishing with us?
Contact book.department@intechopen.com

Numbers displayed above are based on latest data collected.
For more information visit www.intechopen.com



Combined myocardial motion estimation and segmentation using variational techniques

N. Carranza-Herrezuelo¹, A. Bajo^{2,3}, C. Santa-Marta⁴, G. Cristóbal¹,
A. Santos^{2,3} and M. J. Ledesma-Carbayo^{2,3}

¹ Instituto de Óptica (CSIC)

² Biomedical Image Technologies, ETSI Telecomunicación. Universidad Politécnica de Madrid

³ Centro de Investigación Biomédica en Red en Bioingeniería, Biomateriales y Nanomedicina (CIBER-BBN)

⁴ Departamento de Física Matemática y Fluidos. Universidad Nacional de Educación a Distancia
Spain

1. Introduction

One of the most important challenges in the last few years in the medical imaging analysis field has been automatic cardiac motion estimation, to obtain indicators of heart disease. The visualization and quantification of the heart motion is an important aid for an early diagnosis of heart pathologies (Santos & Ledesma-Carbayo, 2006).

In the last few years, there have been numerous technological progresses in non-invasive cardiac imaging methods (Axel & Dougherty, 1989; McVeigh & Atalar, 1992; Fischer et al., 1993; Atalar & McVeigh, 1994; Fischer et al., 1994; Zerhouni et al., 1998). Therefore, there are new clinical options for cardiac illnesses diagnosis (Thomson et al., 2004). Coronary angiography, nuclear imaging, echocardiography and computerized tomography provide most of the information required by the cardiologist and cardiovascular surgeon (Sinitsyn, 2001). In the 80s, magnetic resonance imaging (MRI) was only used for the evaluation of the heart anatomy. Lately, great advances have been achieved, which have totally changed the possibilities of the diagnosis in this area (de Roos et al., 1999; Pohost et al., 2000; Duerden et al., 2006). Some of the facts that have made magnetic resonance imaging a functional and flexible modality are the increment in temporal and spatial resolution, the improvement in signal to noise ratio and the removal of motion artefacts due to motion. Currently, cardiac magnetic resonance (CMR) is considered the reference gold standard to evaluate ventricular function. The acquisition is dynamic, so several frames are acquired in a cardiac cycle. Tissues can be clearly defined without the use of contrast agents, and unlike other tomographic techniques, it can provide images in the desired plane without limitations due to the body anatomy. There are no limitations for the angulation of the images.

Nevertheless, there are still limitations obtaining cardiac function measurements because the myocardial tracking is hindered as there are no intramural features (Axel et al., 2005). With conventional magnetic resonance imaging (MRI) or ultrasound imaging, a qualitative estimation of the local cardiac motion can be done. Nevertheless, it is quite difficult to compare the results obtained among different modalities even by experts. The reference technique to evaluate quantitatively the contractile myocardial function is tagged magnetic resonance imaging (tagged MRI) (Axel & Dougherty, 1989; Prince & McVeigh, 1992; Dornier et al., 2004; Sampath & Prince, 2007). Changing the tissue magnetization, a lineal grid can be superimposed to the myocardium. The tagged grid acts as an intramural intrinsic feature of the tissue until it vanishes due to the T1 relaxation is the process by which the longitudinal magnetization attains its equilibrium value. The time constant to approach the equilibrium value is called T1 of the cardiac muscle. Therefore, the grid moves with the myocardium during the cardiac cycle and cardiac motion can be tracked by means of the grid. As the grid is deforming during the cardiac cycle, the material coordinates can be tracked and motion can be quantified inside the myocardium. The myocardial displacement field and the parameters derived from it, such as strain, have revealed to be very useful for the diagnosis of different pathologies (Lelieveldt et al., 2004).

The most important clinical application for the local functional cardiac analysis is the assessment of the affected but recoverable regions of an ischemic heart (Picano et al., 1991; Nagel et al., 1999). This is usually done by measuring the width of the cardiac wall on CINE images of the myocardium (Lieberman et al., 1981; Götte et al., 2001). However, the myocardial strain calculation implies the accurate computation of the myocardial displacement field.

The methods proposed for motion estimation from tagged images are based on the use of different aspects of the heterogeneity of the myocardium intensity (Axelo et al., 2005). These methods include: tracking the lines of minimum intensity (Guttman et al., 1994; Chen & Amini, 2001; Quian et al., 2003), optical flow (Prince & McVeigh, 1992; Denney & Prince, 1994; Dougherty et al., 1999) or harmonic phase methods (HARP) (Osman et al., 1999).

The methods based on tracking the tags with minimum intensity use an intensity profile model of a grid line. These methods are normally very time consuming, and depend on a user who manually starts to identify the location of the tagging lines in the first frame. Afterwards, the most probable location is searched, or a segmentation using approximations such as morphological operators (Guttman et al., 1994; Young, 1998; Chen & Amini, 2001), tuned filters (Young, 1998; Chen & Amini, 2001), Gabor filters (Quian et al., 2003), deformable grids (Kumar & Goldof, 1993) and manually identified points (Young & Axel, 1992). Although the techniques using tuned filters and Gabor filters are relatively robust to the intensity loss of the tag lines, the limitation of the methods which perform the tracking of lines is that the temporal correspondences are only valid for those pixels belonging to the lines and not for those within them (Axel et al., 2005).

The advantage of the optical flow methods is that they provide a dense estimation of the motion field in two dimensions, and not only a sparse set of data. Technical details about this type of methods will be explained later. Nevertheless, there have been several strategies to perform the tracking of lines in the myocardium using such techniques (Prince & McVeigh, 1992; Gupta & Prince, 1995; Gupta et al., 1997; Dougherty et al., 1999). The main limitation of these methods is the difficulty to follow large displacements.

Phase harmonic methods are based upon the fact that tagged magnetic resonance imaging typically presents a set of different spectral peaks in the Fourier domain corresponding to the spatial frequency of the tag lines. Each peak contains information about the motion perpendicular to the tag line (Zhang et al., 1996). The inverse Fourier transform of one of those peaks is a complex image whose phase is directly related to a directional component of the real motion (Osman et al., 1999; Osman et al., 2000).

Nevertheless, the assessment of myocardial function not only requires the motion estimation but also the segmentation of the myocardium over a cardiac cycle (Chenoune et al., 2005). Identifying the heart chambers, the endocardium and the epicardium is of great importance for clinical applications. Such information can be used to improve the diagnostics of cardiovascular diseases, to estimate the ventricular blood volume, wall mass, wall motion and wall thickening properties (Paragios, 2002). Numerous cardiac segmentation methods have been developed and used to estimate the myocardial boundaries accurately and efficiently. Among these, the two main approaches for cardiac segmentation are based on boundaries, either of an explicit implementation (Montagnat & Delingette, 2005) or an implicit approach such as level sets (Paragios, 2002; Chenoune et al., 2005) or regions (Blekas et al., 2005).

Active contour models have also been very effective in segmenting and tracking moving objects in image sequences, such as cardiac image sequences. Leymarie et al. (Leymarie & Levine, 1993) used the previously segmented contour as an initial seed contour for the current frame to track the contour through a sequence of images. Inspired on this, Gupta et al. (Gupta et al., 1993) proposed an automatic contour propagation scheme throughout the entire slices and frames in their four-dimensional cardiac analysis study using image sequences from MRI. Chalana et al. (Chalana et al., 1996) investigated the dependency of the accuracy of cardiac segmentation on the initial seed contour and proposed a multiple active contour model to reduce the propagation error in sequential segmentation of myocardial boundaries on echocardiographic sequences, by adding temporal smoothness and monotonic motion constraints to the internal and external energy formulation. Li et al. (Li et al., 2002) also proposed a similar approach to take into account a temporal smoothness of the contour.

Regarding the coupling of segmentation and motion estimation, many researchers have addressed this problem. In (Wang & Adelson, 1994), they first estimate local motion and subsequently segment regions with respect to estimated motion. In (Nagel & Enkelmann, 1986; Black & Anandan, 1996; Kornprobst et al., 1999; Weickert & Schnörr, 2001), they propose to model motion discontinuities implicitly by non-quadratic robust estimators. Others tackled the problem of segmenting motion by treating first the motion estimation in disjoint sets and then by optimizing the motion boundaries separately (Schnörr, 1992; Black, 1994; Caselles & Coll, 1996; Paragios & Deriche, 2000). Other approaches are based on Markov Random Field formulations and optimization schemes, such as stochastic relaxation by Gibbs sampling, split-and-merge techniques, deterministic relaxation, graph cuts or expectation maximization (Cremers & Soatto, 2005). A novel variational approach for segmenting an image plane into a set of regions of parametric motion, based on a conditional probability for the spatio-temporal image gradient is presented in (Cremers & Soatto, 2005). In the case of segmentation of cardiac images, several examples can be mentioned where the optical flow has been included into the segmentation process (Giachetti et al., 1996; Mikic et al., 1998).

In this chapter, a new approach is presented which combines the advantages of the variational technique for motion estimation with the segmentation process of the endocardial and epicardial borders by means of a variational-based approach: the well-known level set technique (Li et al., 2005). For endocardial and epicardial border segmentation, dual CINE and tagged cardiac magnetic resonance sequences have been used. A idea was not to develop a new segmentation technique but to implement a hybrid approach that would benefit from the motion estimation of the variational technique, in order to build a more robust implementation for both tagged and conventional cardiac magnetic resonance imaging. The motion estimation technique is based on a variational approach, improved by taking into account the particular features of tagged magnetic resonance sequences. Specifically, this variational method has been enhanced by adding a robustness term based on the accurate tracking at some control points by means of their phase stability. The main idea of the integration of the two sub-systems is to minimize computational cost of the segmentation process together with a better accuracy of the segmentation.

In section 2, we describe the method implemented for segmentation (level sets), for motion estimation (variational techniques) and the hybrid technique for motion estimation and segmentation. Section 3 explains the experiments performed to evaluate and validate the method, and the results obtained. Finally, in section 4, the main conclusions are presented.

2. Methods

2.1 Level Set Segmentation

The level set method technique was introduced by Osher and Sethian (Osher & Sethian, 1988), and later it has been investigated to cope with different image segmentation problems in several publications. The method proposed for the segmentation of the temporal sequence of tagged cardiac magnetic resonance images is a modified version of the variational formulation of the geometric active contours principle proposed by (Li et al., 2005). The main idea is to evolve the boundary C from some initial curve in the direction of the negative energy gradient. This is done by implementing the gradient descent equation (Cremers et al., 2007):

$$\frac{\partial C}{\partial t} = -\frac{\partial E(C)}{\partial C} = F \cdot \mathbf{n} \quad (1)$$

and modelling the evolution along the normal \mathbf{n} with a speed function F . In the implicit contour representation theory, the contour C is represented as the zero level line of some embedding function ϕ such as

$$C(t) = \{(x, y) | \phi(t, x, y) = 0\} \quad (2)$$

In the method proposed by Osher and Sethian in (Osher & Sethian, 1988), a contour is propagated by evolving a time-dependent embedding function ϕ according to an appropriate partial differential equation. Having a contour C evolving along the normal \mathbf{n} with a speed F and since $\phi(C(t), t) = 0$, this equation can be derived as

$$\frac{d}{dt} \phi(C(t), t) = \nabla \phi \frac{\partial C}{\partial t} + \frac{\partial \phi}{\partial t} = \nabla \phi (F \cdot \mathbf{n}) + \frac{\partial \phi}{\partial t} = 0 \quad (3)$$

The evolution equation of the level set function ϕ can be written in the following general form, inserting the definition of the normal $n = \frac{\nabla \phi}{|\nabla \phi|}$

$$\frac{\partial \phi}{\partial t} = -|\nabla \phi|F \quad (4)$$

which is called the level set equation (Osher & Sethian, 1988). Nevertheless, the level set function ϕ can suffer of transients, very sharp and/or flat shape during the evolution. For this reason, it is necessary to initialize the function ϕ as a signed distance function before the evolution starts, and then “reshape” (or “re-initialize”) the function ϕ to be a signed distance function periodically during the evolution. Re-initialization has been extensively used as a numerical remedy in traditional level set methods (Caselles et al., 1993; Malladi et al., 1995). The standard re-initialization method solving the following equation is

$$\frac{\partial \phi}{\partial t} = \text{sign}(\phi_0)(1 - |\nabla \phi|) \quad (5)$$

where ϕ_0 is the function to be re-initialized, and $\text{sign}(\phi)$ is the sign function. There has been copious literature on re-initialization methods (Peng et al., 1999; Sussman & Fatemi, 1999), and most of them are variants of the above partial differential equation (PDE)-based method. Unfortunately, if ϕ_0 is not smooth or ϕ_0 is much steeper on one side of the border than the other, the zero level set of the resulting function ϕ can be moved incorrectly with respect to the original function. Moreover, when the level set function is far away from a signed distance function, these methods may not be able to re-initialize properly the level set function to a signed distance function. In practice, the evolving level set function can deviate greatly from its value as signed distance in a small number of iteration steps, especially when the time step is not chosen small enough. So far, re-initialization has been extensively used as a numerical remedy for maintaining stable curve evolution and ensuring desirable results. From the practical point of view, the re-initialization process can be quite complicated, expensive, and have subtle side effects.

In this chapter we have used the variational approach explained in (Li et al., 2005), which can be easily implemented by a simple finite difference scheme without the need of re-initialization. Provided that a signed distance function must satisfy the desirable property of $|\nabla \phi| = 1$, the minimization of the following integral is proposed

$$P(\phi) = \int_{\Omega} \frac{1}{2} (|\nabla \phi| - 1)^2 dx dy \quad (6)$$

With the above defined functional $P(\phi)$, it is proposed the following variational formulation

$$E(\phi) = \mu P(\phi) + E_m(\phi) \quad (7)$$

where $\mu > 0$ is a parameter controlling the effect of penalizing the deviation of ϕ from a signed distance function, and $E_m(\phi)$ is a certain energy that would drive the motion of the zero level curve of ϕ (Li et al., 2005).

2.2 Proposed Method for Motion Estimation of Tagged Cardiac Magnetic Resonance Images

The method proposed for the study of the motion in tagged CMR is one of the well-known differential techniques. The basis of these methods is the constancy of the intensity structures of local time-varying image regions under motion, at least for a short duration time (Horn & Schunk, 1981). The use of this method actually assumes intensity conservation between consecutive frames, that can be admitted in the case of tagged MR image frames separated by short time intervals as compared with T1 recovery (Ledesma-Carbayo et al., 2008). However, if required, the T1 signal modulation could also be included in the criterion (Ledesma-Carbayo et al., 2008). Let us remember the optical flow constraint equation:

$$\mathbf{v}(x_1, x_2) \cdot \nabla I(x_1, x_2, t_0) + I_t(x_1, x_2, t_0) = 0 \quad (8)$$

where $\mathbf{v} = (v_1, v_2)$, $I_t = \partial I / \partial t$ and $v_1 = \partial x_1 / \partial t$ and $v_2 = \partial x_2 / \partial t$ are the components of the velocity field. This equation needs an additional constraint, as the problem is undetermined (ill posed). The one adopted here is based on the regularization of the velocity fields (Aubert, 1999). The problem originally proposed has to deal with the following energy minimization, proposed by Horn & Schunk in (Horn and Schunk, 1981)

$$\min_v \int_{\Omega} (\mathbf{v} \cdot \nabla I + I_t)^2 dx + \alpha^r \int_{\Omega} (\|\nabla v_1\|^2 + \|\nabla v_2\|^2) dx \quad (9)$$

and modified later on with more robust norms to cope with optical flow discontinuities (Aubert & Kornprobst, 2006)

$$\int_{\Omega} \phi(\|\nabla v_1\|) dx + \int_{\Omega} \phi(\|\nabla v_2\|) dx \quad (10)$$

where the functions ϕ allow noise removal and edge preservation. Among the different ϕ functions (Deriche et al., 1995), in this approach the norm L^1 has been chosen. It is also called Total Variation (TV), $\phi(t) = t$. Very good anisotropic denoising properties of the TV semi-norm are well known (Sroubek & Flusser, 2005). Since TV is highly nonlinear and non continuous, a special attention must be paid to its discretization. Several relaxed linearization schemes were proposed. We follow the half-quadratic regularization scheme describe in (Charbonnier et al., 1997) that introduces an auxiliary variable.

On the other hand in homogeneous areas characterized by low image gradients magnitude, no visible motion can be locally detected. To minimize this undesirable motion, an extra term is added to equation (11) such as

$$\int_{\Omega} c(x) \|\mathbf{v}\|_2^2 dx \quad (11)$$

where $\|\cdot\|_2$ is the Euclidean norm, and

$$c(x) = \frac{1}{\sqrt{\left(\frac{\partial}{\partial x_1} I\right)^2 + \left(\frac{\partial}{\partial x_2} I\right)^2 + \epsilon}} \quad (12)$$

represents a penalizing function, which is small for high image gradients and big for low image gradients. Finally, including the different terms, the energy minimization equation that we propose to use has the following form:

$$\min_v \int_{\Omega} (\mathbf{v} \cdot \nabla I + I_t)^2 dx + \alpha^r \int_{\Omega} \phi(\|\nabla \mathbf{v}\|) dx + \alpha^c \int_{\Omega} c(x) \|\mathbf{v}\|_2^2 dx \quad (13)$$

In the same way that the homogeneous term $c(x)$ has been added, it is easy to add other terms in order to adapt the algorithm to the problem. The main idea of the improved version described here has been introducing a regularization term in order to find a more accurate optical flow based on prior robust estimates in given control points. The new term is going to have information of the displacement of several points inside the myocardium with a very low phase difference with respect to the following frame (estimated below 10^{-3}). For the sequel, we will name these points as control points. Such term has the following form,

$$\beta \sum_i (v_i - p_i) \quad (14)$$

where \mathbf{p}_i is the set of control points. The parameter β is a mask, with non-zero values only for the control point position. The final equation yields as

$$\min_v \int_{\Omega} (\mathbf{v} \cdot \nabla I + I_t)^2 dx + \alpha^r \int_{\Omega} \phi(\|\nabla \mathbf{v}\|) dx + \alpha^c \int_{\Omega} c(x) \|\mathbf{v}\|_2^2 dx + \beta \sum_i (\mathbf{v}_i - \mathbf{p}_i)^2 \quad (15)$$

With this equation, a compromise agreement is reached. The regularization term is going to provide a more accurate optical flow in the neighbourhood of the control points. In those regions without any control point, this term does not have any effect. Although the equation (15) seems to have an easy implementation, obtaining the control points is a challenging task. The tags of the image are an essential property which will allow obtaining such points. There are some papers which propose tracking the dark lines as finding points of minimum intensity (Guttman et al., 1994; Young, 1998; Chen & Amini, 2001). In this case, several tag line points could be chosen as control points. However, the tag fading is a limitation for these techniques, as the error allowed in the displacement estimation of those points has to be very small.

In contrast, techniques using the phase of the images (for instance, the Harmonic Phase or HARP technique reported in (Osman et al., 1999; Osman et al., 2000)) turn out to be very accurate for tracking a selected number of points, that is those points whose phases are not affected by noise and where tag jumping is avoided. As we only need a reduced set of points and not a dense optical flow for these control points, the control points will be a set of points with high stability of phase.

In 1-1 SPAMM (Spatial Modulation of Magnetization) tagging pulse sequences, tags are created with a sinusoidal cross-sectional intensity profile. At any point on or between the tags, the tissue has both the magnetization intensity and the spatial phase of the periodic tag magnetization pattern, which are dependent on position (Axel et al., 2005). So, when the heart moves, a particular piece of tissue has the same phase in the deformed state as it has in the reference state. The phase of those images is an intrinsic invariant property that can be tracked.

As the phase of the tagged images is restricted to be in the range $[-\pi, +\pi]$, the control points will be selected among a set of points in the myocardium having a certain phase, using the criterion explained before to reject the points which phase difference with respect to the following frame is higher than 10^{-3} . This process is fully automatic and it does not need any manual interaction. We are going to select one point per tag intersection, forming a grid of selected points in the myocardium. An example can be seen in Fig. 1.

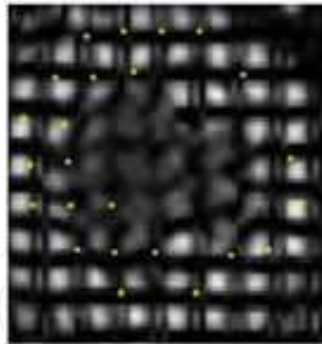


Fig. 1. Example of the control points manually chosen in one of the sequences tested.

From those points, a similar procedure as reported in (Osman et al., 1999) and (Osman et al., 2000) is established for tracking the points, using the Newton-Raphson method. The Newton-Raphson method is a well-known technique to find the root of a function. We are going to apply it in a small region centered in the point of interest, to find the roots in the difference of phase images. To avoid tag jumping, the Newton-Raphson method is only run in a small window around each point, taking into account tag spacing. In addition to that, those points whose difference of phases has an error higher than 10^{-3} have been rejected. Therefore, only points with very good phase stability have been chosen as control points. This automatic selection provides control points with robust tracking estimates including prior information very valid to enhance the method. In principle it does not matter which points are selected, although it is desirable that they are evenly distributed. It is also important to note that the computational time does not increase very much as only a few points are going to be selected.

Another important point is that the control points are different for each pair of images. Thus, the errors which could have been made in previous images of the sequence will not be propagated.

The motion estimation method has been validated with a simulated sequence without noise and with four different levels of Gaussian noise, and also with five real sequences. According to the standardized myocardial division of segments (Cerqueira, Weissman et al. 2002), the myocardium has been divided into six regions, and four points of each region have been manually tracked. Overall, 24 points have been selected along each sequence. The results obtained with the motion estimation method have been compared with the points tracked manually. The error has been computed, as the average root mean square error for each segment. The average root mean square error for synthetic sequences is 0.49 pixels/frame and for real sequences it is 0.62 pixel/frame. Results have been compared to a reference method (HARP), achieving always better results (Carranza-Herrezuelo, 2009a; Carranza-Herrezuelo et al, 2009b).

2.3 Integration of the Motion Estimation and Segmentation Approach

This algorithm has been applied on four sequences where both CINE and tagged CMR images are available (see an example in Fig. 2). The motion field has been extracted for each pair of tagged CMR images. This motion field has been computed with the enhanced variational method, and integrated with the segmentation technique.

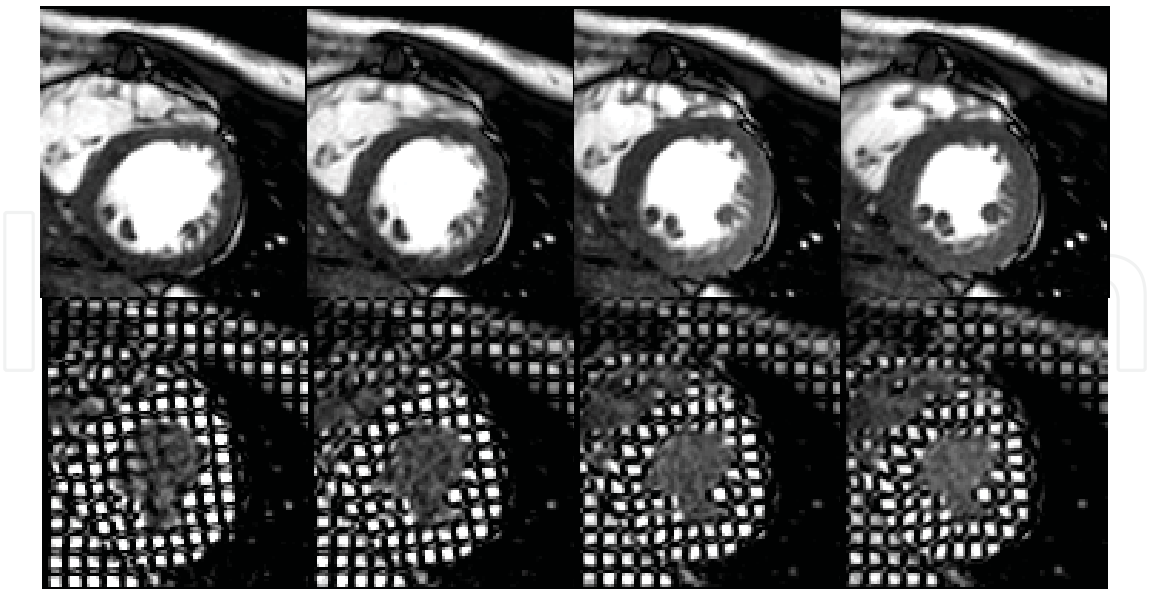


Fig. 2. Cine and tagged CMR images corresponding to the same patient.

To starting the algorithm, the segmentation of the first image is performed being initialized with a manually drawn curve. All the rest operations are automatically accomplished. After the first image is segmented, the next step is to estimate the motion field that applied to this first segmentation will provide the new contour in the next image of the sequence. When the curve for the next image is estimated, the level set technique is run only to refine the solution and for smoothing the first approach. The segmentation algorithm is run on the CINE sequences, while the motion estimation is run on the tagged sequences. The block diagram of the previous steps is shown in Fig. 3

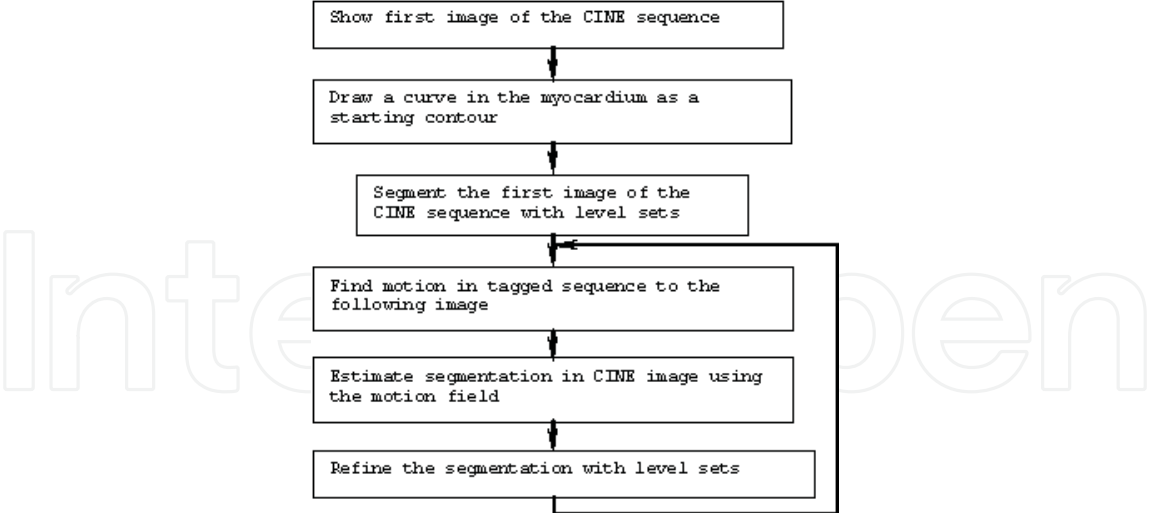


Fig. 3. Block diagram of the system of the motion estimation and segmentation for dual sequences

By means of this algorithm, the computational time of the segmentation is considerably reduced, because we only need to compute the segmentation for the first image of the

sequence. For the rest, the iterative process of the segmentation is stopped when the evolution of the level-set implementation is below a given threshold.

3. Experimental Results

3.1 Experiments

The four sequences were acquired with a Philips Intera 1.5 T (Philips Medical Systems, The Netherlands) using a five element phased-array coil dedicated to cardiac imaging. CINE MR scans were acquired using a breath hold Balanced Fast Field Echo (B-FEE) sequence, obtaining images with a pixel size between 1 mm² and 1.3 mm². As in the previous experiment the tagging sequence used consists of an enhanced version of the SPAMM sequence provided by the manufacturer for our Phillips Intera scanner (Santa-Marta et al., 2006). Both CINE and Tagged MR sequences were acquired using exactly the same acquisition geometry in order to have precise alignment and pixel correspondence between both datasets. Some small rigid misalignments due to the acquisitions in different respiratory positions have been corrected between both sequences before applying the segmentation approach.

The values of the parameters used in the program have been selected manually, choosing the parameters which provided better results. For the motion estimation, the parameters used for the tagged CMR sequences are $\alpha^c = 10^{-8}$, $\alpha^r = 10^{-7}$ and $\beta = 10^{-7}$. The parameter that controls the number of iterations explained in the previous section has been set as 3.8 pixels for the endocardium and 0.5 for the epicardium segmentation. The rest of the parameters employed in the algorithm are the same as stated in (Li et al., 2005).

The computational time has been tested in this experiment. On the other hand, the accuracy of the segmentation has been evaluated. For this purpose the endocardium and epicardium have been manually segmented, independently on each sequence. Four sequences have been analysed selecting the systolic period, and 46 curves from 23 images were manually segmented. To compare the results obtained with the automatic algorithm, the metrics proposed in (Chalana & Kim, 1997) have been used, as described in the following paragraphs.

Let us suppose that we have two curves A and B where the former A is obtained by the segmentation algorithm and the later B is the one manually segmented. Both curves are divided into a set of points, a_i and b_i . In our case, we have used all the points of the contour. The minimum distance of each of the points to the other curve is computed, which is the distance to the closer point in the other curve.

$$d(a_i, B) = \min_j \|b_j - a_i\| \quad (16)$$

In each image of the sequence, the following measures are obtained:

- Mean distance between curves. It is obtained from the distances of all the points

$$d(A, B) = \frac{1}{m} \sum_{i=1}^n d(a_i, B) \quad (17)$$

- Hausdorff distance. Maximum distance of one curve to the other, measured as the maximum value between the distances of all the points.

$$e(A, B) = \max(\max_j \{d(a_i, B)\}, \max_j \{d(b_i, A)\}) \quad (18)$$

- **Overlapping.** From the surfaces defined by the curves, the overlapping degree is the division of the number of coincident pixels in both surfaces, and the number of pixels belonging to one or another.

$$Overlapping(A,B)=\frac{A\cap B}{A\cup B} \tag{19}$$

An example of the manually and automatic segmentation in two different frames is shown in Figs. 4-5. It can be seen how the contours are smoother in the case of the automatic segmentation (see e.g. Fig. 4c-d).

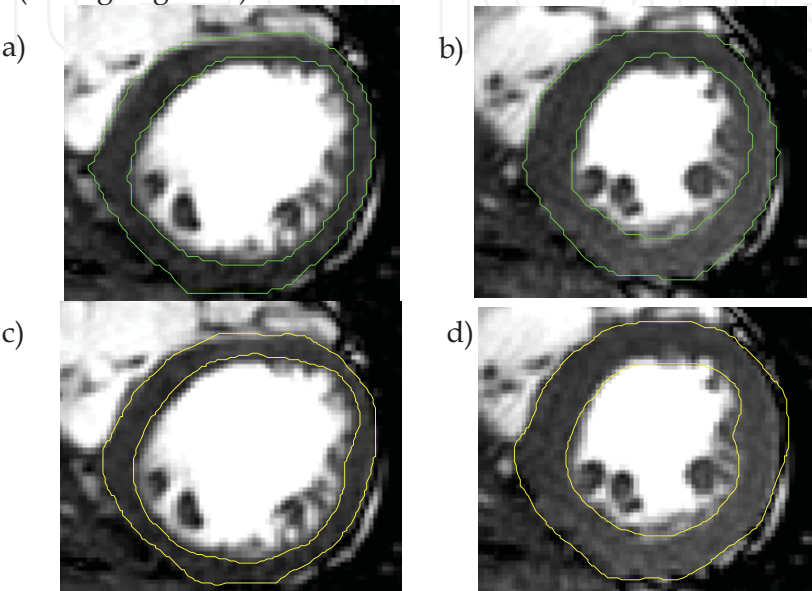
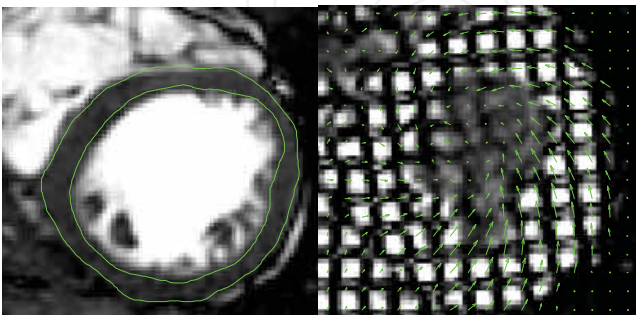


Fig. 4. a) and b) Example of manually segmentation. c and d) Example of automatic segmentation.

3.2 Results

The results obtained for one of the sequences are visualized in Fig. 5., where the segmentation result (left column) and the optical flow (right column) on the tagged images are shown.



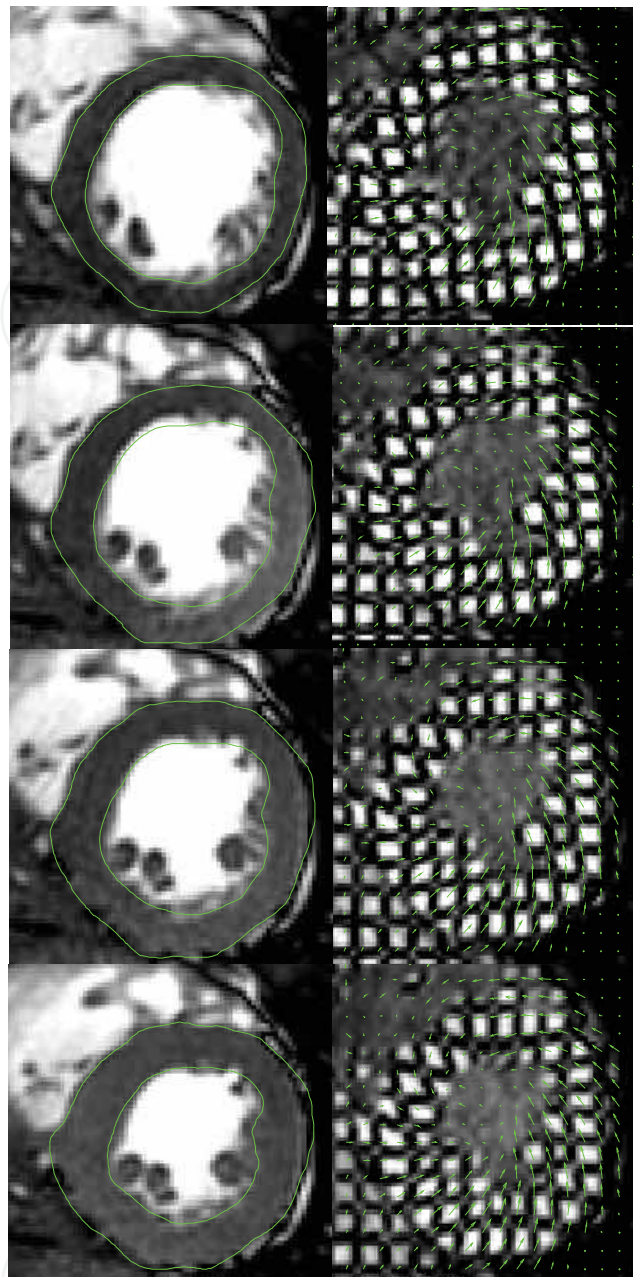


Fig. 5. Segmentation results and optical flow for the first five images of the sequence. The first column shows the CINE images with the segmentation and the second column shows the optical flow obtained with the tagged CMR images.

As it can be seen, the results obtained adjust well to the endocardium and epicardium. The contour fit perfectly to the myocardial border, avoiding the inclusion of the papillary muscles which can not be achieved so easily on the tagged images. Fig. 6 shows the results of the computational time. As it can be seen in figure 6, the computational time for the integrated solution is smaller than the one needed if the sequence were segmented frame by frame. Fluctuations on the computational time for the integrated method are due only to the refinement of the segmentation needed for each frame; this fact explains the increase of the computational time between frames forth and fifth.

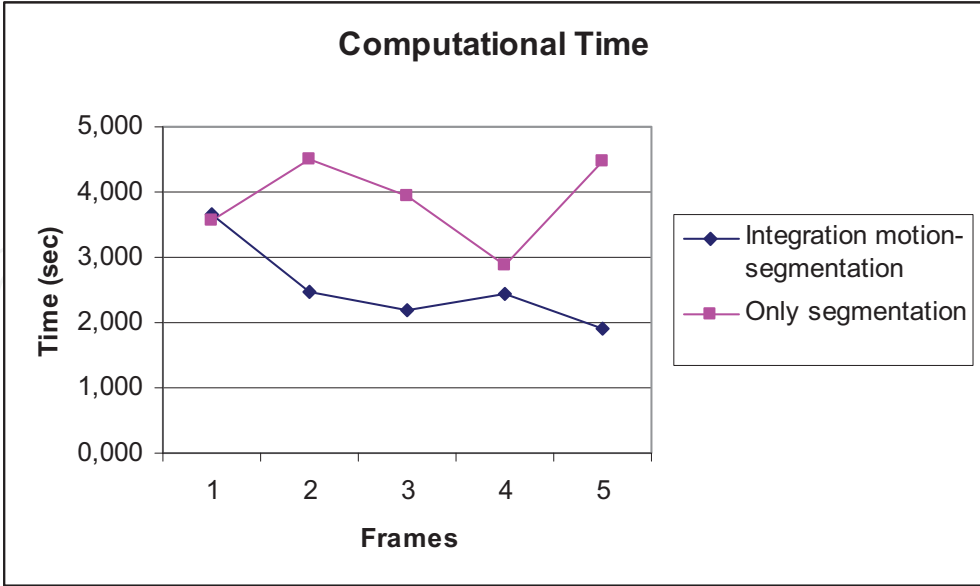


Fig. 6. Computational time for the proposed integrated solution compared with the time obtained segmenting each image for the dual sequence.

The results of the evaluation of the 46 curves tested are shown in Table 1. Resultant parameters show that the segmentation performance is very accurate.

		Mean Distance (pixels) Mean ± SD	Hausdorff Distance (pixels) Mean ± SD	Overlapping degree (%) Mean ± SD
Sequence 1	Endocardium	0.94 ± 0.9	2.71 ± 1.44	90 ± 3.84
	Epicardium	1.01 ± 0.04	2.80 ± 0.21	93 ± 1.85
Sequence 2	Endocardium	1.25 ± 0.16	3.75 ± 0.97	88 ± 4.04
	Epicardium	0.96 ± 0.00	2.65 ± 0.40	94 ± 0.59
Sequence 3	Endocardium	0.87 ± 0.18	2.82 ± 0.33	87 ± 3.12
	Epicardium	0.82 ± 0.31	2.60 ± 0.70	92 ± 2.93
Sequence 4	Endocardium	0.88 ± 0.43	2.35 ± 1.09	90 ± 6.01
	Epicardium	1.24 ± 0.22	3.54 ± 0.74	90 ± 1.62

Table 1. Evaluation results of the segmentation (mean distance, Hausdorff distance and overlapping degree) for the four sequences tested in comparison to manual delineations.

The mean distance between pixels is always below 1.25 pixels, and the Hausdorff distance is smaller than 4 pixels. In the first sequence, results for the endocardium and epicardium segmentation are similar. In the second sequence, the results obtained for the epicardium are better. This is due to the fact the manual segmentation of the endocardium is generally quite difficult. In the second sequence, the resolution of the images was lower than in the first case, and the error obtained with the segmentation algorithm is a bit higher than those obtained in the first sequence.

4. Conclusions

A method for segmentation and motion estimation of the myocardium based on level sets and variational techniques has been presented. The segmentation method uses a level set method implemented through a variational formulation, which has been integrated with a motion estimation algorithm, also based on variational techniques. This approach applied to dual sequences takes advantage of the appealing features from each type of images (detail resolution from CINE CMR and motion estimation from Tagged MR). The segmentation has been proved to be feasible in real images, having a low computational cost. On the other hand the accuracy of the segmentation has been tested in dual CINE + Tagged MR sequences in comparison to manual delineation of the endocardium and epicardium. Results show a good performance of the algorithm with a mean error between curves of approximately one pixel. The proposed approach constitutes a very interesting framework for the measurement of global and regional functional parameters from both types of data (CINE+tagged MRI).

5. Acknowledgments

This research has been supported by the following grants: TEC2007-67025/TCM, TEC2006-28009-E, TEC2007-30709E TIN2007-68048-C02-01, CDTI-CDTEAM and SINBAD (PS-010000-2008-1) by the Spanish Ministry of Science and Innovation.

6. References

- Atalar, E. & McVeigh, E. R. (1994). Minimization of dead-periods, *Magnetic Resonance in Medicine*, Vol. 32, No. 6, (773-777), 0740-3194
- Aubert, G. & Kornprobst, P. (2006). *Mathematical Problems in Image Processing. Partial Differential Equations and the Calculus of Variations*, Springer, 978-0-387-32200-1
- Aubert, G.; Deriche, R. & Kornprobst, P. (1999). Computing optical flow via variational techniques, *Siam Journal on Applied Mathematics*, Vol. 60, No. 1, (156-182), 0036-1399
- Axel, L. & Dougherty, L. (1989). MR imaging of motion with spatial modulation of magnetization, *Radiology*, Vol. 171, (841-845), 1527-1315
- Axel, L.; Montillo, A. & Kim, D. (2005). Tagged magnetic resonance imaging of the heart: a survey, *Medical Image Analysis*, Vol. 9, No. 4, (376-393), 1361-8415
- Black, M. J. (1994). Recursive non-linear estimation of discontinuous flow fields, *Proceedings of the European Conference of Computer Vision*, Vol. 800, (138-145).
- Black, M. J. & Anandan, P. (1996). The robust estimation of multiple motions: Parametric and piecewise-smooth flow fields, *Computer Vision of Graphical Image Processing*, Vol. 63, No. 1, (75-104), 0734-189X
- Blekas, K.; Likas, A.; Galatsanos, N. & Lagaris, I. (2005). A spatially constrained mixture model for image segmentation, *IEEE Transactions on Neural Networks*, Vol. 16, No. 2, (494-498), 1045-9227
- Carranza-Herrezuelo, N. (2009a). *New Contributions on Motion Estimation through Optical Flow Techniques Applied to Cardiac Magnetic Resonance Imaging*, PhD Thesis, Universidad Politécnica de Madrid

- Carranza-Herrezuelo, N. ; Bajo, A.; Sroubek, F.; Santa-Marta, C.; Cristóbal, G.; Santos, A. & Ledesma-Carbayo, M. J. (2009b). Motion estimation of Tagged Cardiac Magnetic Resonance Images using Variational Techniques, *Computerized Medical Imaging and Graphics*, 0895-6111, under review
- Caselles, V.; Catte, F.; Coll, T. & Dibos, F. (1993). A Geometric Model for Active Contours in Image Processing, *Numerische Mathematik*, Vol. 66, No.1, (1-31), 0945-3245
- Caselles, V. & Coll, B. (1996). Snakes in movement, *SIAM Journal on Numerical Analysis*, Vol. 33, (2445-2456), 0036-1429
- Cerqueira, M. D.; Weissman, N. J.; Dilsizian, V.; Jacobs, A. K.; Kaul, S.; Laskey, W. K.; Pennell, D. J.; Rumberger, J. A.; Ryan, T. & Verani, M. S. (2002). Standardized Myocardial Segmentation and Nomenclature for Tomographic Imaging of the Heart: A Statement for Healthcare Professionals from the Cardiac Imaging Committee of the Council on Clinical Cardiology of the American Heart Association, *Journal of the American Heart Association*, Vol. 105, (539-542), 0194911X
- Cremers, D.; Rousson, M. & Deriche, R. (2007). A review of statistical approaches to level set segmentation: Integrating color, texture, motion and shape, *International Journal of Computer Vision*, Vol. 72, No. 2, (195-215), 0920-5691
- Cremers, D. & Soatto, S. (2005). Motion Competition: A Variational Approach to Piecewise Parametric Motion Segmentation, *International Journal of Computer Vision*, Vol. 62, No. 3, (249-265), 0920-5691
- Chalana, V. & Kim, Y. (1997). A methodology for evaluation of boundary detection algorithms on medical images, *IEEE Transactions on Medical Imaging*, Vol. 16, No. 5, (642-652), 0278-0062
- Chalana, V.; Linker, D. T.; Haynor, D. R. & Kim, Y. M. (1996). A multiple active contour model for cardiac boundary detection on echocardiographic sequences, *IEEE Transactions on Medical Imaging*, Vol. 15, No. 3, (290-298), 0278-0062
- Charbonnier, P.; BlancFeraud, L.; Aubert, G. & Barlaud, M. (1997). Deterministic edge-preserving regularization in computed imaging, *IEEE Transactions on Image Processing*, Vol. 6, No. 2, (298-311), 1057-7149
- Chen, Y. S. & Amini, A. A. (2001). A MAP framework for tag line detection in SPAMM data using Markov random fields on the B-spline solid, *Proceedings of IEEE Workshop on Mathematical Methods in Biomedical Image Analysis*, 9780818673672
- Chenoune, Y.; Delechelle, E.; Petit, E.; Goissen, T.; Garot, J. & Rahmouni, A. (2005). Segmentation of cardiac cine-MR images and myocardial deformation assessment using level set methods, *Computerized Medical Imaging and Graphics*, Vol. 29, No.8, (607-616), 0895-6111
- de Roos, A.; Kunz, P.; Lamb, H.; Kroft, L.; Langerak, S.; Doornbos, J. & van der Wall, E. (1999). Magnetic resonance imaging of ischemic heart disease: Why cardiac magnetic resonance imaging will play a significant role in the management of patients with coronary artery disease, *Journal of Computer Assisted Tomography*, Vol. 23, (S135-S141), 03638715
- Denney, T. & Prince, J. L. (1994). Optimal brightness functions for optical flow estimation of deformable motion, *IEEE Transactions on Image Processing*, Vol. 3, No. 2, (178-191), 1057-7149
- Deriche, R.; Kornprobst, P. and Aubert, G. (1995). Optical-Flow Estimation while Preserving its Discontinuities: A Variational Approach, *Invited Session Papers from the Second*

- Asian Conference on Computer Vision: Recent Developments in Computer Vision*, Vol. 1035, (71 – 80)
- Dornier, C.; Somsen, A.; Ivancevic, M. K.; Osman, N. F.; Didier, D.; Righetti, A. & Vallée, J. P. (2004). Comparison between tagged MRI and standard cine MRI for evaluation of left ventricular ejection fraction, *Radiology*, Vol. 14, (1348-1352), 1527-1315
- Dougherty, L.; Asmuth, J.; Blom, A.; Axel, L. & Kumar, R. (1999). Validation of an optical flow method for tag displacement estimation, *IEEE Transactions on Medical Imaging*, Vol. 18, No. 4, (359-363), 0278-0062
- Duerden, R. M.; Pointon, K. S. & Habib, S. (2006). Review of clinical cardiac MRI, *Imaging*, Vol. 18, (178-186), 0942-8925
- Fischer, S. E.; McKinnon, G. C.; Maier, S. E. & Boesiger, P. (1993). Improved myocardial tagging contrast, *Magnetic Resonance in Medicine*, Vol. 30, (191-200), 0740-3194
- Fischer, S. E.; McKinnon, G. C.; Scheidegger, M. B.; Prins, W.; Meier, D. & Boesiger, P. (1994). True myocardial motion tracking, *Magnetic Resonance in Medicine*, Vol. 31, (401-413), 0740-3194
- Giachetti, A., Gigli, G. & Torre, V. (1996). Computer assisted analysis of echocardiographic image sequences, *Medical Image Analysis*, Vol. 2, No. 4, (261-284), 1361-8415
- Götte, M. J. W.; van Rossum, A. C.; Twisk, J. W. R.; Kuijter, J. P. A.; Marcus, J. T. & Visser, C. A. (2001). Quantification of regional contractile function after infarction: strain analysis superior to wall thickening analysis in discriminating infarct from remote myocardium, *Journal of American College of Cardiology*, Vol. 37, (808-817), 0735-1097
- Gupta, A.; Vonkurowski, L.; Singh, A.; Geiger, D.; Liang, C. C.; Chiu, M. Y.; Adler, L. P.; Haacke, M. & Wilson, D. L. (1993). Cardiac Mr Image Segmentation Using Deformable Models, *Proceedings of Computers in Cardiology*, (747-750), 0276-6574
- Gupta, S. N. & Prince, J. L. (1995). On variable brightness optical flow for tagged MRI, *Information Processing in Medical Imaging: 14th International Conference.*, (323-334), Dordrecht: Kluwer, June 1995
- Gupta, S. N.; Prince, J. L. & A-Theotokis, S. (1997). Bandpass optical flow for tagged MR imaging, *Proceedings of IEEE International Conference of Image Processing*, (364-367), San Diego, October 1997
- Guttman, M. A.; Prince, J. L. & McVeigh, E. R. (1994). Tag and Contour-Detection in Tagged MR-Images of the Left-Ventricle, *IEEE Transactions on Medical Imaging*, Vol. 13, No. 1, (74-88), 0278-0062
- Horn, B. K. P. & Schunk, B. G. (1981). Determining Optical-Flow, *Artificial Intelligence*, Vol. K17, No. 1-3, (185-203), 1989-1660
- Kornprobst, P.; Deriche, R. & Aubert, G. (1999). Image sequence analysis via partial differential equations, *Journal of Mathematical Image Vision*, Vol. 11, No. 1, (5-16), 1573-7683
- Kumar, S. & Goldof, D. (1993). Automatic tracking of SPAMM grid and the estimation of deformation parameters from cardiac MR images, *IEEE Transactions on Medical Imaging*, Vol. 13, No. 1, (122-132), 0278-0062
- Ledesma-Carbayo, M. J.; Derbyshire, J. A.; Sampath, S.; Santos, A.; Desco, M. & McVeigh, E. R. (2008). Unsupervised estimation of myocardial displacement from tagged MR sequences using nonrigid registration, *Magnetic Resonance in Medicine*, Vol. 59, (181-189), 0740-3194

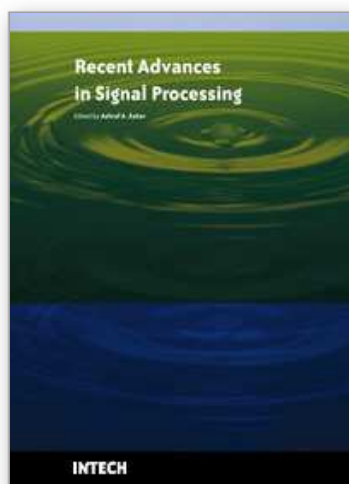
- Lelieveldt, B. P. F., Van der Geest, R. J. & Reiber, J. H. C. (2004). Towards 'One-Stop' Cardiac MR Image Analysis, *Image Decisions MRI*, Vol. 8, No.2, (2-12), 1433-3317
- Leymarie, F. & Levine, M. D. (1993). Tracking Deformable Objects in the Plane Using an Active Contour Model, *IEEE Transactions on Pattern Analysis and Machine Intelligence*, Vol. 15, No. 6, (617-634), 0018-9340
- Li, C. M.; Xu, C. Y.; Gui, C. & Fox, M. D. (2005). Level set evolution without re-initialization: A new variational formulation, *Proceedings of IEEE Computer Society Conference on Computer Vision and Pattern Recognition*, Vol. 1, (430-436), 0-7695-2372-2
- Li, M.; Kambhamettu, C. & Stone, M. (2002). Motion-based post processing of deformable contours, *Proceedings of The Indian Conference on Computer Vision, Graphics and Image Processing (ICVGIP)*, Ahbedamad (India), December 2002.
- Lieberman, A. N.; Weiss, J. L.; Jugdutt, B. I.; Becker, L. C.; Bulkley, B. H.; Garrison, J. G.; Hutchins, G. M.; Kallman, C. A. & Weisfeldt, M.L. (1981). Two-dimensional echocardiography and infarct size: relationship of regional wall motion and thickening to the extent of myocardial infarction in the dog, *Circulation*, Vol. 63, (739-746), 0009-7322
- Malladi, R.; Sethian, J. A. & Vemuri, B. C. (1995). Shape Modeling with Front Propagation - A Level Set Approach, *IEEE Transactions on Pattern Analysis and Machine Intelligence*, Vol. 17, No. 2, (158-175), 0018-9340
- McVeigh, E. R. & Atalar E. (1992). Cardiac tagging with breath hold cine MRI, *Magnetic Resonance in Medicine*, Vol. 28, (318-327), 0740-3194
- Mikic, I.; Krucinski, S. & Thomas, J. D. (1998). Segmentation and tracking in echocardiographic images: Active contours guided by optical flow estimates, *IEEE Transactions on Medical Imaging*, Vol. 17, No. 2, (274-284), 0278-0062
- Montagnat, J. & Delingette, H. (2005). 4D deformable models with temporal constraints: applications to 4d cardiac image segmentation, *Medical Image Analysis*, Vol. 9, No. 1, (87-100), 1361-8415
- Nagel, E.; Lehmkuhl, H. B.; Bocksch, W.; Klein, C.; Vogel, U.; Frantz, E.; Ellmer, A.; Dreyse, S. & Fleck, E. (1999). Noninvasive Diagnosis of Ischemia-Induced Wall Motion Abnormalities with the Use of High-Dose Dobutamine Stress MRI: Comparison With Dobutamine Echocardiography Stress, *Circulation*, Vol. 99, (763-770), 0009-7322
- Nagel, H. H. & Enkelmann, W. (1986). An investigation of smoothness constraints for the estimation of displacement vector fields from image sequences, *IEEE Transactions in Pattern Analysis and Machine Intelligence*, Vol. 8, No. 5, (565-593), 0018-9340
- Osher, S. & Sethian, J. A. (1988). Fronts Propagating with Curvature-Dependent Speed - Algorithms based on Hamilton-Jacobi Formulations, *Journal of Computational Physics*, Vol. 79, No. 1, (12-49), 1090-2716
- Osman, N. F.; Kerwin, W. S.; McVeigh, E. R. & Prince, J. L. (1999). Cardiac motion tracking using CINE harmonic phase (HARP) magnetic resonance imaging, *Magnetic Resonance in Medicine*, Vol. 42, No. 6, (1048-1060), 0740-3194
- Osman, N. F.; McVeigh, E. R. & Prince, J. L. (2000). Imaging heart motion using harmonic phase MRI, *IEEE Transactions on Medical Imaging*, Vol. 19, No. 3, (186-202), 0278-0062

- Paragios, N. (2002). A variational approach for the segmentation of the left ventricle in cardiac image analysis, *International Journal of Computer Vision*, Vol. 50, No.3, (546-362), 0920-5691
- Paragios, N. & Deriche R. (2000). Geodesic active contours and level sets for the detection and tracking of moving objects, *IEEE Transactions in Pattern Analysis and Machine Intelligence*, Vol. 22, No.3, (266-280), 0018-9340
- Peng, D.; Merriman, B.; Osher, S.; Zhao, H. & Kang, M. (1999). A PDE-based fast local level set method, *Journal of Computational Physics*, Vol. 155 (410-438), 1090-2716
- Picano, E.; Lattanzi, F.; Orlandini, A.; Marini, C. & L'Abbate, A. (1991). Stress echocardiography and the human factor: the importance of being expert, *Journal of American College of Cardiology*, Vol. 17, (666-669), 0735-1097
- Pohost, G. M.; Biederman, R. W. & Doyle, M. (2000). Cardiovascular magnetic resonance imaging and spectroscopy in the new millennium, *Current Problems in Cardiology*, Vol. 25, No. 8, (525-620), 0146-2806
- Prince, J. L. & McVeigh, E. R. 1992. Motion Estimation from Tagged MR Image Sequences, *IEEE Transactions on Medical Imaging*, Vol. 11, No. 2, (238-249), 0278-0062
- Quian, Z.; Montillo, A.; Metaxas, D. & Axel, L. (2003). Segmenting cardiac MRI tagging lines using Gabor filter banks. *Proceedings of International Conference of the Engineering in Medicine and Biology Society*, Cancun, Mexico
- Sampath, S. & Prince, J. L. (2007). Automatic 3D tracking of cardiac material markers using slice-following and harmonic-phase MRI, *Magnetic Resonance Imaging*, Vol. 25. No. 2, (197-208), 1796-2234
- Santa-Marta, C.; Ledesma-Carbayo, M. J.; Bajo, A.; Pérez-David, E.; Santos, A. & Desco, M. (2006). Respiratory Gated SPAMM Sequence for Magnetic Resonance Cardiac Tagging, *Proceedings of Computers in Cardiology*, September 2006, Valencia (Spain).
- Santos, A. & Ledesma-Carbayo, M. J. (2006). *Cardiac Imaging*. New Jersey, Wiley Encyclopedia of Biomedical Engineering, John Wiley & Sons Inc, 9783131477811
- Schnörr, C. (1992). Computation of discontinuous optical flow by domain decomposition and shape optimization, *International Journal of Computer Vision*, Vol. 8, No. 2, (153-165), 0920-5691
- Sinitsyn, V. (2001). Magnetic resonance imaging in coronary heart disease, *European Journal of Radiology*, Vol. 38, No. 3, (191-199), 1527-1315, 0720-048X
- Sroubek, F. & Flusser, J. (2005). Multichannel blind deconvolution of spatially misaligned images, *IEEE Transactions on Image Processing*, Vol. 14, No. 7, (874-883), 1057-7149
- Sussman, M. & Fatemi, E. (1999). An efficient, interface preserving level set redistancing algorithm and its application to interfacial incompressible fluid flow, *SIAM Journal on Scientific Computing*, Vol. 20, (1165-1191), 1095-7197
- Thomson, L. E. J.; Kim, R. J. & Judd, R. M. (2004). Magnetic resonance imaging for the assessment of myocardial viability, *Journal of Magnetic Resonance Imaging*, Vol. 19, No. 6, (771-788), 1749-8023
- Wang, J. Y. A. & Adelson, E. H. (1994). Representing moving images with layers, *IEEE Transactions on Image Processing*, Vol. 3, No. 5, (625-638), 1057-7149
- Weickert, J. & Schnörr, C. (2001). A theoretical framework for convex regularizers in PDE-based computation of image motion, *International Journal of Computer Vision*, Vol. 45, No. 3, (245-264), 0920-5691

- Young, A. A. (1998). Model tags: Direct 3D tracking of heart wall motion from tagged MR images. *Medical Image Computing and Computer-Assisted Intervention - Miccai'98*. W. M. Wells, A. Colchester and S. Delp., Vol. 1496, (92-101)
- Young, A. A. & Axel, L. (1992). Three-dimensional motion and deformation of the heart wall: Estimation with spatial modulation of magnetization -- A model-based approach, *Radiology*, Vol. 185, (241-247), 1527-1315
- Zhang, S.; Douglas, M.; Yaroslavsky, L.; Summers, R.; Dilsizen, V.; Fananapazir, L. & Bacharach, S. (1996). A Fourier based algorithm for tracking SPAMM tags in gated magnetic resonance cardiac images, *Medical Physics*, Vol. 23, No.8, (1359-1369)

IntechOpen

IntechOpen



Recent Advances in Signal Processing

Edited by Ashraf A Zaher

ISBN 978-953-307-002-5

Hard cover, 544 pages

Publisher InTech

Published online 01, November, 2009

Published in print edition November, 2009

The signal processing task is a very critical issue in the majority of new technological inventions and challenges in a variety of applications in both science and engineering fields. Classical signal processing techniques have largely worked with mathematical models that are linear, local, stationary, and Gaussian. They have always favored closed-form tractability over real-world accuracy. These constraints were imposed by the lack of powerful computing tools. During the last few decades, signal processing theories, developments, and applications have matured rapidly and now include tools from many areas of mathematics, computer science, physics, and engineering. This book is targeted primarily toward both students and researchers who want to be exposed to a wide variety of signal processing techniques and algorithms. It includes 27 chapters that can be categorized into five different areas depending on the application at hand. These five categories are ordered to address image processing, speech processing, communication systems, time-series analysis, and educational packages respectively. The book has the advantage of providing a collection of applications that are completely independent and self-contained; thus, the interested reader can choose any chapter and skip to another without losing continuity.

How to reference

In order to correctly reference this scholarly work, feel free to copy and paste the following:

N. Carranza-Herrezuelo, A. Bajo, C. Santa-Marta, G. Cristobal, A. Santos and M. J. Ledesma-Carbayo (2009). Combined Myocardial Motion Estimation and Segmentation Using Variational Techniques, Recent Advances in Signal Processing, Ashraf A Zaher (Ed.), ISBN: 978-953-307-002-5, InTech, Available from: <http://www.intechopen.com/books/recent-advances-in-signal-processing/combined-myocardial-motion-estimation-and-segmentation-using-variational-techniques>

INTECH
open science | open minds

InTech Europe

University Campus STeP Ri
Slavka Krautzeka 83/A
51000 Rijeka, Croatia
Phone: +385 (51) 770 447
Fax: +385 (51) 686 166
www.intechopen.com

InTech China

Unit 405, Office Block, Hotel Equatorial Shanghai
No.65, Yan An Road (West), Shanghai, 200040, China
中国上海市延安西路65号上海国际贵都大饭店办公楼405单元
Phone: +86-21-62489820
Fax: +86-21-62489821

© 2009 The Author(s). Licensee IntechOpen. This chapter is distributed under the terms of the [Creative Commons Attribution-NonCommercial-ShareAlike-3.0 License](https://creativecommons.org/licenses/by-nc-sa/3.0/), which permits use, distribution and reproduction for non-commercial purposes, provided the original is properly cited and derivative works building on this content are distributed under the same license.

IntechOpen

IntechOpen